Electronic Supplementary Material (ESI) for CrystEngComm.
This journal is © The Royal Society of Chemistry 2022

Electronic Supplementary Information

Non-covalent interactions of hydroperoxo group in crystalline adducts of organic hydroperoxides and their potassium salts

Ivan. A. Buldashov,[a,b] Alexander G. Medvedev,[a] Alexey A. Mikhaylov,[a] Andrei V. Churakov,[a] Ovadia Lev*[c] and Petr V. Prikhodchenko*[a]

[a]Kurnakov Institute of General and Inorganic Chemistry, Russian Academy of Sciences, Leninskii prosp. 31, Moscow 119991, Russia. E-mail: prikhman@gmail.com

[b]Faculty of Chemistry, National Research University Higher School of Economics, Miasnitskaya Str. 20, Moscow 101000, Russia

[c]The Casali Center, The Institute of Chemistry and The Harvey M. Krueger Family Center for Nanoscience and Nanotechnology, The Hebrew University of Jerusalem, Edmond J. Safra Campus, Jerusalem 91904, Israel. E-mail: ovadia@mail.huji.ac.il

Table of contents

Experimental Section

Materials

Cyclohexanone (≥99.0%), 4-Methylcyclohexanone (99%), *tert*-butyl hydroperoxide (70% solution in water), 37% aqueous hydrogen peroxide solution and potassium hydroxide (≥85.0%) were purchased from Sigma-Aldrich. The solvents were dried over molecular sieves (3 Å or 4 Å) and freshly distilled prior use. A solution of *tert*-butyl hydroperoxide in benzene (63 wt%) was prepared from water solution.

Caution! Bishydroperoxides are shock- and friction sensitive and, consequently, should be handled with care.

Synthesis

Geminal bishydroperoxides were prepared from the corresponding ketones by the reaction with hydrogen peroxide according to the published procedure.[1]

Synthesis of $2C_4H_{10}O_2•C_4H_9O_2^-K^+$ (**1**). A dispersion of potassium hydroxide (3.691 g, 55.92 mmol) in 50 ml of benzene was added dropwise to a 63 wt% solution of *tert*-butyl hydroperoxide in benzene (4 g, 27.96 mmol) with stirring at 0-5°C. The reaction mass was stirred for 3 h at room temperature. The potassium hydroxide was separated by filtration, washed by 15 ml of benzene. The collected filtrate was evaporated under vacuum in a rotary evaporator and product was washed two times by cold hexane. The white powder was dried in vacuum dessicator for 0.5 h. Yield 55% (1.575 g). Anal. Calc. for $C_{12}H_{29}O_6K_1$: C, 46.73; H, 9.48. Found: C, 46.45; H, 9.38.

Synthesis of $C_6H_{12}O_4•C_6H_{11}O_4^-K^+$ (**2**). A solution of potassium hydroxide (2.5 mmol, 0.165 g) in 50 ml of ethanol was added dropwise to a solution of 1,1-dihydroperoxycyclohexane (1.25 mmol, 0.185 g) in 50 ml of ethanol with stirring at 0-5°C. The reaction mixture was stirred for 1 h. The 50 ml of ice-cold acetone was added to the clear solution. The precipitate was isolated by filtration and washed with cold acetone. The white powder was dried in vacuum dessicator for 0.5 h. Yield 83% (0.173 g). Anal. Calc. for $C_{12}H_{23}O_8K_1$: C, 43.10; H, 6.93. Found: C, 43.01; H, 6.82.

Synthesis of $C_7H_{14}O_4 \bullet C_7H_{13}O_4^-K^+$ (**3**). A solution of potassium hydroxide (2.5 mmol, 0.165 g) in 50 ml of ethanol was added dropwise to a solution of 1,1-dihydroperoxy-4-methylcyclohexane (1.25 mmol, 0.203 g) in 50 ml of ethanol with stirring at 0-5°C. The reaction mixture was stirred for 1 h. The 50 ml of ice-cold acetone was added to the clear solution. The precipitate was isolated by filtration and washed with cold acetone. The white powder was dried in vacuum dessicator for 0.5 h. Yield 85% (0.192 g). Anal. Calc. for $C_{14}H_{27}O_8K_1$: C, 46.39; H, 7.51. Found: C, 46.29; H, 7.46.

Methods

Elemental analysis. Carbon and hydrogen content were determined using the Perkin-Elmer 2400 series II Analyzer (CHN).

FTIR spectra were recorded on a JASCO FT/IR-4600 spectrometer.

Differential scanning calorimetry (DSC) measurements were performed on differential scanning calorimeter, DSC-60 Plus (Shimadzu) under argon flow at a heating rate of 5 °C/min.

X-ray analysis. Single crystals suitable for X-ray analysis were obtained by slow evaporation of benzene (for **1**) and methanol solution (**2**, **3**). Experimental intensities were measured on a Bruker D8 Venture diffractometer (**1**,**3**) at 100 K and Bruker SMART APEX II (**2**) at 150 K (graphite monochromatized MoK_α radiation, $\lambda = 0.71073$ Å) using ω-scan mode. Absorption corrections based on measurements of equivalent reflections were applied.[2] The structures were solved by direct methods and refined by full matrix least-squares on F^2 with anisotropic thermal parameters for all non-hydrogen atoms.[3] Hydrogen atoms of alkyl fragments in **1-3** were placed in calculated positions and refined using a riding model. Hydrogen atoms of hydroperoxo groups in **1-3** were found from difference Fourier synthesis and refined isotropically. X-ray diffraction studies were performed at the Centre of Shared Equipment of IGIC RAS. Selected crystallographic data for **1**-**3** are provided in Table S2. The crystallographic data for **1-3** have been deposited with the Cambridge Crystallographic Data Centre as supplementary publications under the CCDC numbers 2154003-2154005, respectively.

Computational Method.

Periodic (Solid-State) DFT Followed by Bader Analysis of the Crystalline Electronic Density.

The space groups and unit cell parameters of **1-3** obtained in the single-crystal X-ray studies are fixed and structural relaxations are limited to the positional parameters of atoms. The atomic positions from experiment are used as the starting point in the solid-state DFT computations. Density functional theory computations with periodic boundary conditions (solid-state DFT) were performed in the Crystal17 software package[4] using B3LYP in the localized basis set 6-31G**.[5] The B3LYP/6-31G** approximation provides reliable and consistent results in studying the intermolecular interactions in crystals.[6–8] The mixing coefficient of Hartree-Fock/Kohn-Sham matrices is set to 25%. Tolerance on energy controlling the self-consistent field convergence for geometry optimizations and frequencies computations is set to 10^{-10} and 10^{-11} Hartree, respectively. The shrinking factor of the reciprocal space net is set to 3. The optimized structures are found to correspond to the minimum point on the potential energy surface.

Crystal structure database analysis

The structures with 2 or more hydroperoxide groups located at different carbon atoms are considered here as monohydroperoxides (n = 1). The structures with 2 hydroperoxide groups located at the same carbon atom are defined as geminal dihydroperoxides (n = 2). Metal coordination complexes with -C-O-OH group in a ligand and peroxycarboxylic acids are not considered here. In case of protons of hydroperoxide groups with occupancy ≠ 1.000 the data on H-bonds are presented considering the position of hydrogen atom with the highest occupancy value. The data on each of the -C-O-OH groups are separated by «;» symbol. The data on HB-A are separated by «,» symbol and are given in the following order: -C-O-**O**H, then -C-**O**-OH. The structures that also form inter- or intramolecular HB-A are marked with «§» symbol.

Special cases:

In the structure AWOMOQ, H (-C-O-OH group) atom is localized wrongly.[9]

In the structure DERXAC, the data on one of the nine hydroperoxide groups is not shown since there is erroneously short O-O distance 1.366(6); H (-C-O-OH group) atoms in two hydroperoxide groups are localized wrongly, and parameters of H-bonds involving these atoms are therefore marked with «*» symbol.[10]

In the structure FUFDIT, the data on the angle of H-bond [∠(O_H-H-X)] is not shown since the angle O-O-H (-C-O-OH group) = 86.80° is erroneously small.[11]

The data on the structure REDSEB is not shown since there is wrong refinement of disordered hydroperoxide groups resulting in short O-O (in both disordered -C-O-OH groups with 0.6500 occupancy) distances 1.291(8), 1.299(8).[12]

The data on the structure SOWLAS is not shown since there is erroneously short O-O distance (-C-O-OH group) 1.30(1).[13]

The data on the structure XILRIW is not shown since there is wrong refinement of disordered hydroperoxide groups resulting in short O-O distances 1.25(2) (in -C-O-OH group with disordered O,O' atoms with 0.5000 occupancy), 1.32(2) (in -C-O-OH group with disordered O,O',H atoms with 0.5000 occupancy).[14]

The data on the structure XILRUI is not shown since there is wrong refinement of disordered hydroperoxide group resulting in small angle O-O-H (in -C-O-OH group with disordered O,O',H atoms with 0.5470 occupancy) = 79.6°.[14]

In the structure ZEDLOJ, H (-C-O-OH group) atom is not localized.[15]

† - HB-D is implemented as an intermolecular H-bond with the same organic hydroperoxide molecule

‡ - HB-D is implemented as a H-bond with other type of coformer

Supplementary Tables

Table S1. Structure features of HPCA

№	Refcode	Structure	Stoichiometry	n(HB-D)	X	D(O$_H$—X)	n(HB-A)	Y	D(Y$_H$—X)	Ref
Hydrates										
n = 1 (monohydroperoxides)										
1	AWOMOQ	6-(hydroperoxy(methoxy)methyl)-2-methoxy-3,5-dimethyl-2-(oxiran-2-yl)tetrahydro-2H-pyran-4-yl acetate monohydrate	R-C(OOH)$_n$ • Cof	1	O (water)	2.726(7)	0,0	-	-	9
2	BAMCID	5a,10a-bis(hydroperoxy)octahydro-5H,10H-dipyrrolo[1,2-a:1',2'-d]pyrazine-5,10-dione monohydrate	R-C(OOH)$_n$ • Cof	1; 1	O (water) ; -//-	2.739(3); 2.715(3)	0,0; 0,0	-	-	16
3	FOLRAB	(5-Benzyl-5-hydroperoxy-3-methyl-1,2-dioxolan-3-yl)methanol monohydrate	R-C(OOH)$_n$ • Cof	0[†]	-	-	1,0	O (water)	2.925(1)	17
4	FUFDIT[§]	6-Hydroperoxy-5-hydroxythymine hemihydrate	R-C(OOH)$_n$ • **0.5x** Cof	1; 0[†]	O (water)	2.705(4)	0,0; 0,0	-	-	11
5	FUWQOG[§]	3-benzyl-3-hydroperoxycyclohexane-1,2-diol hemihydrate	R-C(OOH)$_n$ • **0.5x** Cof	1	O (water)	2.700	0,0	-	-	18
6	GEJFOR[§]	Piperazine-2,3,5,6-tetrayl tetrahydroperoxide pyrazine solvate dihydrate	R-C(OOH)$_n$ • **2x** Cof • **2x** pyrazine	1; 0[‡]; 1; 0[‡]	O (water) ; -//-	2.6068(16); -//-	0,0; 0,0; 0,0; 0,0	-	-	19
7	JOPQIQ[§]	3-acetyl-11-hydroperoxy-8-(1H-indol-3-ylmethyl)-2,9,9a-trimethyltetradecahydroazuleno[6,5-	R-C(OOH)$_n$ • Cof	1	O (water)	2.760(4)	0,0	-	-	20

		d]oxireno[f]isoindole-5,6-dione monohydrate								
8	POBVUY[§]	(1S,3S,4S,4aS,4bS,5S,8R,8aS,10aS)-1-bromo-8a-(bromomethyl) -1,2,3,4,4a,4b,5,8,8a,9,10,10a-dodecahydro-5-hydroperoxy -8-isopropyl-4,10a-dimethylphenanthrene-3,4-diol hemihydrate	R-C(OOH)$_n$ • **0.5x** Cof	0[†]; 0[†]	-	-	1,0; 0,0	O (water)	3.083(6)	[21]
9	WELMAE	(8α,9β,11β,14β,16β,23S,24R)-16-Hydroperoxy-11-hydroxy-3-oxo-24,25-epoxydammar-13(17)-en-23-yl acetate	R-C(OOH)$_n$ • Cof	1	O (water)	2.767(12)	0,0	-	-	[22]
n = 2 (geminal dihydroperoxides)										
10	AHEQEL[§]	cyclohexane-1,1,4,4-tetrayl tetrahydroperoxide monohydrate	R-C(OOH)$_n$ • Cof	0[†];1; 0[†];1	O (water); -//-	2.696(2); -//-	1,0;0,0; 1,0;0,0	O (water); -//-	2.7403(13); -//-	[23]
11	OCOYOY	adamantane-2,2-diperoxol monohydrate	R-C(OOH)$_n$ • Cof	1,1	O (water), -//-	2.6612(14); 2.8079(15)	1,0;0,1	O (water); -//-	2.7300(14); 2.7945(15)	[24]
Molecular (metal-)organic compounds with a lone electron pair on oxygen or nitrogen atoms										
n = 1 (monohydroperoxides)										
12	AGAGUL	cis-1,3-Di-t-butyl-2,4-bis(t-butylamino)-1,3,2,4-diazadiphosphetidine 2,4-dioxide cumene alcohol cumene hydroperoxide	R-C(OOH)$_n$ • Cof • CmOH	1	O (P=O group)	2.739(7)	0,0	-	-	[25]
6	GEJFOR[§]	Piperazine-2,3,5,6-tetrayl tetrahydroperoxide pyrazine solvate dihydrate	R-C(OOH)$_n$ • **2x** H_2O • **2x** Cof	0[‡]; 1; 0[‡]; 1	N (pyrazinic); -//-	2.7573(18); -//-	0,0; 0,0; 0,0; 0,0	-	-	[19]
13	MADNIS	dimethyl 2,8,14,20-tetraethyl-2,14-bis(hydroperoxy)-26,28-	R-C(OOH)$_n$ • **2x** Cof	1; 0[†]	O (C=O group)	2.734(3)	0,0; 0,0	-	-	[26]

		dioxoheptacyclo[19.3.1.1^{3,7}.1^{4,24}.1^{9,13}.1^{12,16}.1^{15,19}]triaconta-1(25),3(30),4,6,9(29),10,12,15(27),16,18,21,23-dodecaene-6,18-dicarboxylate acetone solvate								
14	PEPDUJ	α-(9-Anthroyl)-α-(9-anthryloxy)-9-hydroperoxy-10-methylene-9,10-dihydroanthracene diethyl ether solvate	R-C(OOH)$_n$ • Cof	1	O (bridging atom)	2.691(6)	0,0	-	-	27
15	QABFOR§	3-Benzyl-6-hydroperoxy-12-hydroxy-4,5,10,12-tetramethyl-1-oxo-2,3,3a,6,6a,9,10,11,12,15-decahydro-1H-cycloundeca[d]isoindol-15-yl acetate methanol solvate	R-C(OOH)$_n$ • Cof	1	O (C$_{sp}^3$-OH group)	2.723(4)	0,0	-	-	28
16	SOYFIV	9-Methylamino-1H-phenalen-1-one (1,4-dioxan-2-yl hydroperoxide) solvate	R-C(OOH)$_n$ • Cof	1	O (C=O group)	2.659(2)	0,0	-	-	29
17	TEGVUZ	tetraethylammonium {N^2,N^6-bis[2,6-di-isopropylphenyl]pyridine-2,6-dicarboxamidato}-(cumene peroxolato)-copper(ii) bis(cumene hydroperoxide)	R-C(OOH)$_n$ • **0.5x** Cof • **0.5x** Et$_4$N$^+$	1; 1; 1; 1	O (C=O group); -//-; -//-; -//-	2.683(2); 2.618(2); 2.694(2); 2.611(2)	0,0; 0,0; 0,0; 0,0	-	-	30
18	TOYTIN	2,2'-peroxybis(butane-2-peroxol) (ethane-1,2-diyl)bis[oxo(diphenyl)phosphine]	R-C(OOH)$_n$ • Cof	1; 1	O (P=O group); -//-	2.627(3); -//-	0,0; 0,0	-	-	31
19	WAGVEI	(2,2-dimethyl-1,3-dioxolane-4,5-	R-C(OOH)$_n$ • **6.67x** Cof •	1	O (C$_{sp}^3$-	2.818(13)	0,0	-	-	32

		diyl)bis(diphenylmethanol) 4,4a,5,6,7,8-hexahydronaphthalen-2(3H)-one 4a-hydroperoxy-4,4a,5,6,7,8-hexahydronaphthalen-2(3H)-one	**5.67x** $C_{10}H_{14}O$		OH group)				
20	ZEDLOJ	5-Hydroperoxy-2,4,4,6-tetraphenyl-4,5-dihydropyrimidine acetone solvate	R-C(OOH)$_n$ • Cof	1	O (C=O group)	2.578(6) /2.895(6) (*The acetone solvent molecule is disordered over two sets of equivalent positions*)	0,0	-	-	15
21	ZIGNOU	N-(5-(Isopropyl(methyl)amino)-2-(2-oxo-3-((6-(trifluoromethyl)quinazolin-4-yl)amino)pyrrolidin-1-yl)cyclohexyl)acetamide tetrahydrofuran-2-yl hydroperoxide	R-C(OOH)$_n$ • Cof	1	N ((C_{sp^2},C_{sp^2})N fragment)	2.6819	0,0	-	-	33
22	ZOKYUV	2-(isopropyldiazenyl)propan-2-yl hydroperoxide 1-isopropyl-2-isopropylidenehydrazine	R-C(OOH)$_n$ • Cof	1	N (C=$\underline{\text{N}}$-N fragment)	2.7609(8)	1,0	N ((N,C_{sp^3}) $\underline{\text{N}}$H fragment)	3.1736(8)	34
n = 2 (geminal dihydroperoxides)									
23	BAFGEX	Propane-2,2-diyl dihydroperoxide tricyclohexylphosphine oxide	R-C(OOH)$_n$ • Cof	1;1	O (P=O group); -//-	2.7197(15); 2.6769(14)	0,0;0,0	-	-	35
24	BAFGIB	Propane-2,2-diyl dihydroperoxide	R-C(OOH)$_n$ • Cof	1;1	O (P=O	2.6864(14); 2.7715(15)	0,0;0,0	-	-	35

		triphenylphosphine oxide			group); -//-					
25	CURVUI	diazido-(2,2'-bipyridine)-dihydroxo-platinum(iv) bis(propane-2,2-diyl dihydroperoxide)	R-C(OOH)$_n$ • **0.5x** Cof	1;1; 1;1	O (Pt-OH group); -//-; -//-; -//-	2.726(2); 2.769(2); 2.702(2); 2.805(2)	0,0;0,0; 0,0;0,0	-	-	36
26	REDSAX	propane-2,2-diyl dihydroperoxide methylenebis(diphenylphosphine) dioxide	R-C(OOH)$_n$ • Cof	1;1	O (P=O group); -//-	2.742(2); 2.816(2)	0,0;0,0	-	-	12
27	REDSIF	butane-2,2-diyl dihydroperoxide triphenylphosphine oxide	R-C(OOH)$_n$ • Cof	1;1; 1;1	O (P=O group); -//-; -//-; -//-	2.706(3); 2.734(3); 2.720(3); 2.747(3)	0,0;0,0; 0,0;0,0	-	-	12
28	REDSOL	1-phenylethane-1,1-diyl dihydroperoxide tricyclohexylphosphine oxide	R-C(OOH)$_n$ • Cof	1;1	O (P=O group); -//-	2.7193(15); 2.6645(15)	0,0;0,0	-	-	12
29	REDSUR	pentane-3,3-diyl dihydroperoxide ethane-1,2-diylbis(diphenylphosphine) dioxide	R-C(OOH)$_n$ • **0.5x** Cof	1;1	O (P=O group); -//-	2.751(2); 2.827(2)	0,0;0,0	-	-	12
30	REDTAY	cyclohexane-1,1-diyl dihydroperoxide tricyclohexylphosphine oxide	R-C(OOH)$_n$ • Cof	1;1	O (P=O group); -//-	2.705(1); 2.723(1)	0,0;0,0	-	-	12
31	REDTEC01	pentane-3,3-diyl dihydroperoxide tricyclohexylphosphine oxide	R-C(OOH)$_n$ • Cof	1;1	O (P=O group); -//-	2.679(2); 2.687(1)	0,0;0,0	-	-	12
32	RIHQOR	6,6'-dimethyl-2,2'-bipyridine-N,N'-dioxide propane-2,2-diperoxol solvate	R-C(OOH)$_n$ • **0.5x** Cof	1; 1	O (N$^+$-O$^-$ group); -//-	2.943(1); 2.662(1)	0,0;0,0	-	-	37
33	VUTFUO	cyclohexane-1,1-diperoxol tris(4-methylphenyl)(oxo)-	R-C(OOH)$_n$ • Cof	1;1	O (P=O group);	2.7038(15); 2.7579(14)	0,0;0,0	-	-	38

		phosphine			-//-					
34	VUTGAV	cyclohexane-1,1-diperoxol tris(2-methylphenyl)(oxo)-phosphine	R-C(OOH)$_n$ • Cof	1;1	O (P=O group); -//-	2.686(2); 2.720(3)	0,0;0,0	-	-	38
35	VUTGEZ	cycloheptane-1,1-diperoxol tris(4-methylphenyl)(oxo)-phosphine	R-C(OOH)$_n$ • Cof	1;1	O (P=O group); -//-	2.7849(17); 2.6889(17)	0,0;0,0	-	-	38
36	VUTGID	cycloheptane-1,1-diperoxol tris(2-methylphenyl)(oxo)-phosphine	R-C(OOH)$_n$ • Cof	1;1	O (P=O group); -//-	2.7057(16); 2.7245(16)	0,0;0,0	-	-	38
37	XAHMIC	Ethane-1,2-diylbis(diphenylphosphine) dioxide bis(propane-2,2-diyl dihydroperoxide)	R-C(OOH)$_n$ • **0.5x** Cof	1;1	O (P=O group); -//-	2.758(2); 2.824(3)	0,0;0,0	-	-	39
	XAHMIC01			1;1; 1;1	O (P=O group); -//-; -//-; -//-	2.7562(19); 2.8084(19); 2.794(2); 2.711(2)	0,0;0,0; 0,0;0,0			35
38	XILROC	Tricyclohexylphosphine oxide bis(hydroperoxy)cyclopentane	R-C(OOH)$_n$ • Cof	1;1	O (P=O group); -//-	2.766(3); 2.697(4)	0,0;0,0	-	-	14
39	OCOYUE	adamantane-2,2-diperoxol tris(4-methylphenyl)(oxo)phosphane	R-C(OOH)$_n$ • Cof	1,1	O (P=O group)	2.748(10); 2.69(2)	0,0;0,0	-	-	24
40	OCOZAL	adamantane-2,2-diperoxol tris(2-methylphenyl)(oxo)phosphane	R-C(OOH)$_n$ • Cof	1,1	O (P=O group)	2.781(4); 2.712(3)	0,0;0,0	-	-	24
41	OCOZEP	adamantane-2,2-diperoxol tricyclohexyl(oxo)phosp	R-C(OOH)$_n$ • Cof	1,1	O (P=O group)	2.680(7); 2.706(7)	0,0;0,0	-	-	24

		hane								
Alkali metal salts										
n = 1 (monohydroperoxides)										
42	DERKET	(tert-butyl hydroperoxide)-(tert-butyl peroxolato)-(1,4,7,10-tetramethyl-1,4,7,10-tetraazacyclododecane)-sodium tert-butyl hydroperoxide solvate	$\mathrm{Na^+}$ • $\mathrm{{}^tBuOO^-}$ • $\mathrm{{}^tBuOOH}$ • $\mathrm{(MeN(CH_2)_2)_4}$ • **2x** $\mathrm{{}^tBuOOH}$	1; 1; 1	O (C-O-$\underline{\mathrm{O}}^-$ group); O (C-O-$\underline{\mathrm{O}}$H group); O (C-O-$\underline{\mathrm{O}}$-group)	2.642(5); 2.640(7); 2.410(5)	0,0; 0,0; 1,0	O (C-O-OH group)	2.640(7)	10
43	DERWUV	(cumene peroxolato)-(1,4,7,10-tetramethyl-1,4,7,10-tetraazacyclododecane)-lithium cumene hydroperoxide solvate	$\mathrm{Li^+}$ • $\mathrm{CmOO^-}$ • $\mathrm{(MeN(CH_2)_2)_4}$ • CmOOH	1; 1	O (C-O-$\underline{\mathrm{O}}^-$ group); -//-	2.51(1); 2.522(9)	0,0; 0,0	-	-	10
44	DERXAC	tris(tert-butyl hydroperoxide)-(tert-butyl peroxolato)-(1,4,7,10-tetramethyl-1,4,7,10-tetraazacyclododecane)-potassium bis(tert-butyl hydroperoxide)-(tert-butyl peroxolato)-(1,4,7,10-tetramethyl-1,4,7,10-tetraazacyclododecane)-potassium tert-butyl hydroperoxide solvate	$\mathrm{K^+}$ • $\mathrm{{}^tBuOO^-}$ • **3x** $\mathrm{{}^tBuOOH}$ • $\mathrm{(MeN(CH_2)_2)_4}$ • **2x** $\mathrm{K^+}$ • **2x** $\mathrm{{}^tBuOO^-}$ • **4x** $\mathrm{{}^tBuOOH}$ • **2x** $\mathrm{(MeN(CH_2)_2)_4}$ • **2x** $\mathrm{{}^tBuOOH}$	1; 1; 1; 1; 1; 1*; 1*; 1	O (C-O-$\underline{\mathrm{O}}^-$ group); -//-; O (C-O-$\underline{\mathrm{O}}$H group); O (C-O-$\underline{\mathrm{O}}^-$ group); -//-; O (C-O-$\underline{\mathrm{O}}$H group)*; -//-*; O (C-O-$\underline{\mathrm{O}}^-$ group)	2.625(5); 2.445(4); 2.654(5); 2.619(5); 2.429(5); 2.621(5)*; 2.598(5)*; 2.436(4)	0,0; 1,0; 0,0; 0,0; 1,0*; 0,0; 0,0; 1,0*	O (C-O-OH group); -//-*; -//-*	2.654(5); 2.621(5)*; 2.598(5)*	10
45	MUKTUI	(μ_3-Hydroxo)-(μ_2-tert-butyl peroxolato-O,O,O',O')-(μ_2-tert-butyl peroxolato-O,O,O')-	$\mathrm{Ga^{3+}}$ • **2x** $\mathrm{Li^+}$ • **2x** $\mathrm{{}^tBuOO^-}$ • $\mathrm{OH^-}$ • **2x** $\mathrm{HC(SiMe_3)_2^-}$ •	1	O (C-O-$\underline{\mathrm{O}}^-$ group)	2.568(4)	0,0	-	-	40

		bis(bis(trimethylsilyl)methyl)-(tert-butyl hydroperoxide-O,O')-gallium-di-lithium hexane solvate	^{t}BuOOH • **0.25x** C_6H_{14}							
46	MUKVAQ	bis(μ_2-tert-butyl peroxolato-O,O,O',O')-bis(tert-butyl hydroperoxide-O,O')-di-lithium	**2x** Li^+ • **2x** ^{t}BuOO$^-$ • **2x** ^{t}BuOOH	1; 1	O (C-O-$\underline{O}^-$ group); -//-	2.531(1); -//-	0,0; 0,0	-	-	40
47	CCDC2154003	bis(tert-butyl hydroperoxide) (tert-butyl peroxolato) potassium	K^+ • ^{t}BuOO$^-$ • **2x** ^{t}BuOOH	1; 1	O (C-O-$\underline{O}^-$ group); -//-	2.469(2); 2.569(2)	0,0; 0,0	-	-	a)
n = 2 (geminal dihydroperoxides)										
48	CCDC2154004	(cyclohexane-1,1-dihydroperoxide) (cyclohexane-1,1-hydroperoxoperoxolato) potassium	K^+ • $C_6H_{11}O_4^-$ • $C_6H_{12}O_4$	1,1	O (C-O-$\underline{O}^-$ group), -//-	2.614(3); 2.435(3)	1,1	O (C-O-OH group), -//-	2.614(3); 2.435(3)	a)
49	CCDC2154005	(4-methylcyclohexane-1,1-dihydroperoxide) (4-methylcyclohexane-1,1-hydroperoxoperoxolato) potassium	K^+ • $C_7H_{13}O_4^-$ • $C_7H_{14}O_4$	1,1; 1	O (C-O-$\underline{O}^-$ group), -//-; -//-	2.533(2); 2.605(2); 2.598(2)	0,0; 0,0	-	-	a)

a) Current study

Table S2. X-ray structure determination summary

Compound	**1**	**2**	**3**
Empirical formula	$2C_4H_{10}O_2{\bullet}C_4H_9O_2^-K^+$	$C_6H_{12}O_4{\bullet}C_6H_{11}O_4^-K^+$	$C_7H_{14}O_4{\bullet}C_7H_{13}O_4^-K^+$
F_w	308.45	334.40	362.45
Crystal system	Orthorhombic	Orthorhombic	Monoclinic
Space group	$P2_12_12_1$	*Pccn*	$P2_1/c$
a/Å	8.5398(3)	24.9888(10)	15.4395(12)
b/Å	11.8631(4)	6.3547(3)	10.8481(9)
c/Å	17.8926(7)	9.8148(4)	10.6569(8)
$\alpha/^o$	90	90	90
$\beta/^o$	90	90	99.627(3)
$\gamma/^o$	90	90	90
V/Å^3	1812.67(11)	1558.55(12)	1759.8(2)
Z	4	4	4
F(000)	672	712	776
d_{calc}/g•cm^{-3}	1.130	1.425	1.368
μ/mm^{-1}	0.31	0.375	0.338
T/K	100	150	100
Data collected	15894	16071	15973
Unique data (R_{int})	3954 (0.042)	2262 (0.032)	4227 (0.049)
Reflections with $I>2\sigma(I)$	3521	2061	3287
θ range/°	2.06-26.99	3.26-29.99	2.31-25.24
No of variables	190	143	268
R_1 [$I>2\sigma(I)$]	0.034	0.056	0.047
wR_2 (all data)	0.064	0.142	0.094
GOF	1.049	1.191	1.090
$\Delta\rho_{max,min}$/e Å^{-3}	0.17 / -0.19	1.04 / -0.83	0.30 / -0.30

Table S3. Experimental and optimized parameters of the O-H…O H-bonds in **3-5** at the B3LYP/6-31G** level of theory.

Fragment	*R*(O…O), Å	*R*(O-H), Å	*R*(H…O), Å	∠(O-H…O),°
3				
O(4)-H(4)…O(2)	2.533(2)/2.547	0.98(3)/1.026	1.56(3)/1.522	176(2)/177.6
O(6)-H(6)…O(2)	2.605(2)/2.608	0.86(3)/1.011	1.77(3)/1.615	165(3)/166.2
O(8)-H(8)…O(2)	2.598(2)/2.583	0.86(3)/1.011	1.74(3)/1.578	176(3)/171.8
4				
O(2)-H(2)…O(1)	2.723(1)/2.694	0.850/0.994	1.880/1.703	175.2/168.8
O(5)-H(5)…O(1)	2.705(1)/2.677	0.850/0.995	1.860/1.695	170.6/174.6
5				
O(3)-H(3)…O(1)	2.628(4)/2.644	0.850/0.995	1.860/1.668	149.7/165.9
O(4)-H(4)…O(1)	2.760(4)/2.746	0.850/0.983	1.920/1.780	179.1/166.6

Table S4. Selected crystallographic parameters of hydroperoxo groups of 1-3

Compound	**1**	**2**	**3**
torsion ∠(C-O-O-H), °	109.5(18), 105.5(18)	112(5), 132(3)	141.1(16), 103(2), 88(2)
∠(O-O-H), °	96.8(18), 99.6(17)	98(5), 93(3)	96.9(15), 98(2), 99(2)
R(O-O), Å	1.473(2), 1.475(2)	1.478(2), 1.474(2)	1.4728(18), 1.463(2), 1.459(3)

Table S5. Computed values of the electron density, ρ_b, the local electronic kinetic energy density, G_b, at the O…O critical point, the H-bond enthalpy, $-\Delta H_{HB}$, and energy, E_{HB}, evaluated using Eqs. (1) and (2), respectively.

Fragment	$-\Delta H_{HB}$, kJ mol^{-1}	ρ_b (a.u.)	G_b (a.u.)	E_{HB}, kJ mol^{-1}
3				
O(4)-H(4)…O(2)	**41.8**	0.0738	0.0546	**61.4**
O(6)-H(6)…O(2)	**34.8**	0.0582	0.0430	**48.3**
O(8)-H(8)…O(2)	**37.4**	0.0639	0.0481	**54.1**
4				
O(2)-H(2)…O(1)	**29.6**	0.0448	0.0334	**37.6**
O(5)-H(5)…O(1)	**30.1**	0.0431	0.0335	**37.6**
5				
O(3)-H(3)…O(1)	**31.0**	0.0476	0.0370	**41.6**
O(4)-H(4)…O(1)	**25.5**	0.0370	0.0277	**31.1**

Table S6. Computed values of the electron density, ρ_b, the Laplacian of the electron density, $\nabla^2\rho_b$, the local electronic kinetic energy density, G_b at the K…O critical point and energy, E_{KO}, evaluated using Eq. (2).

R(K…O), Å	ρ_b (a.u.)	$\nabla^2\rho_b$ (a.u.)	G_b (a.u.)	E_{KO}, kJ mol^{-1}
2.721	0.0164	0.0763	0.0165	**18.5**
2.776	0.0146	0.0661	0.0142	**16.0**
2.780	0.0148	0.0654	0.0142	**16.0**
2.797	0.0140	0.0628	0.0134	**15.1**
2.927	0.0109	0.0473	0.0100	**11.2**
2.947	0.0095	0.0429	0.0089	**10.0**
3.377	0.0035	0.0178	0.0033	**3.7**

Supplementary Figures

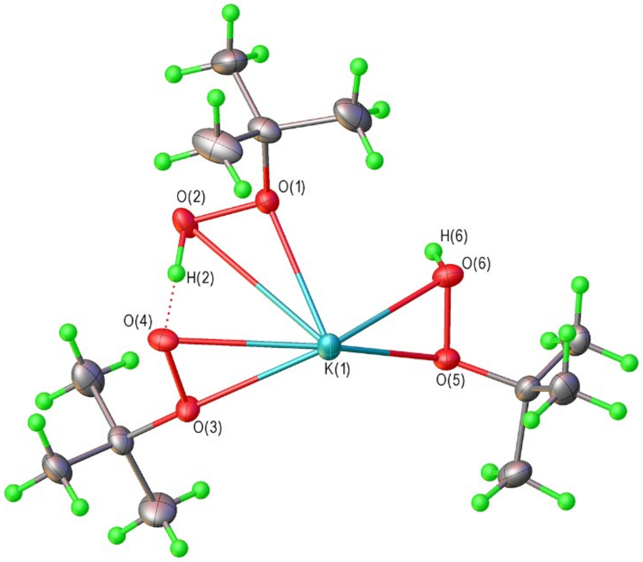

Fig. S1 Asymmetric unit in the structure of **1**. Displacement ellipsoids are drawn at 50% probability level. H-bond is shown as dashed line.

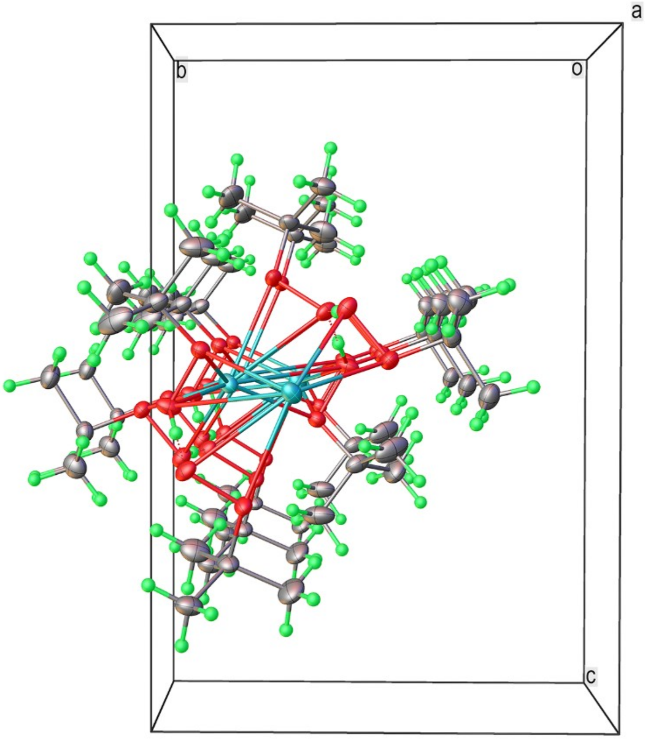

Fig. S2 The infinite chains in **1** along the *a* axis. H-bonds are shown as dashed lines. Displacement ellipsoids are drawn at the 50% probability level.

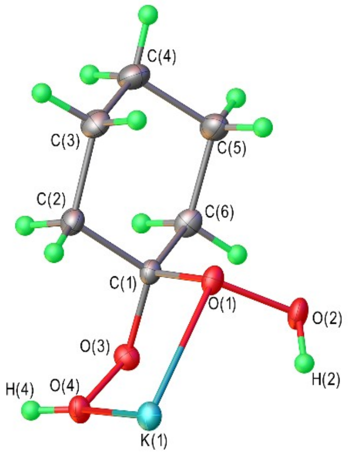

Fig. S3 Asymmetric unit in the structure of **2**. Displacement ellipsoids are drawn at 50% probability level.

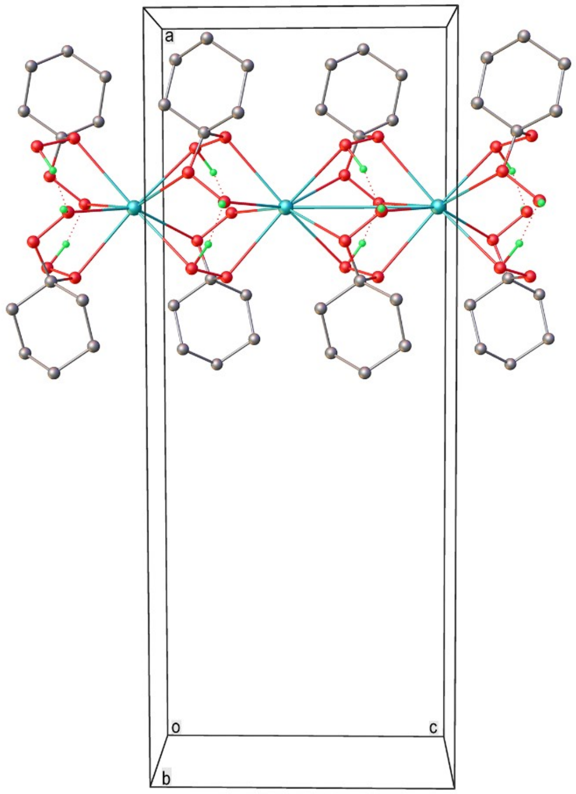

Fig. S4 The infinite chains in **2** along *c* axis. H-bonds are shown as dashed lines.

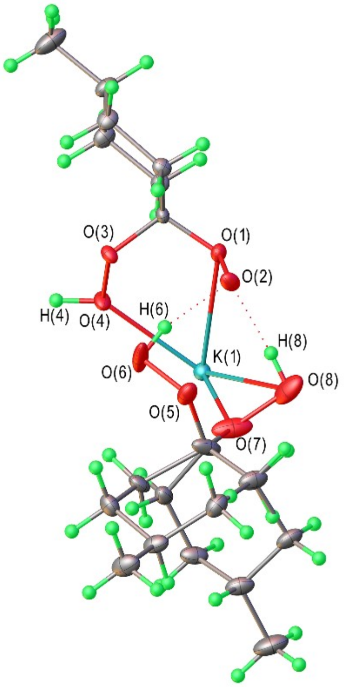

Fig. S5 Asymmetric unit in the structure of **3**. Displacement ellipsoids are drawn at 50% probability level. H-bonds are shown as dashed lines.

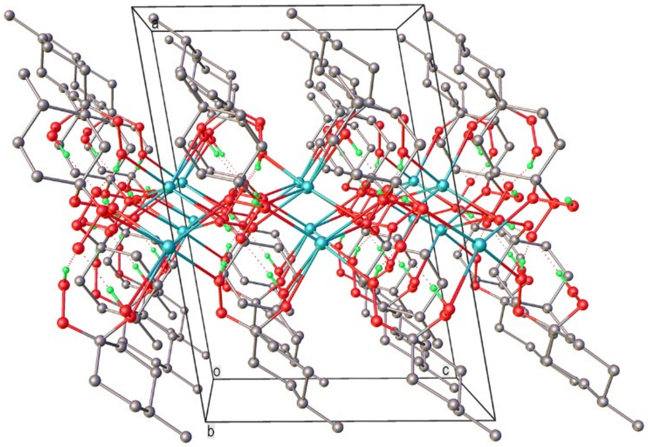

Fig. S6 Layers perpendicular to the *a* axis in **3**. H-bonds are shown as dashed lines.

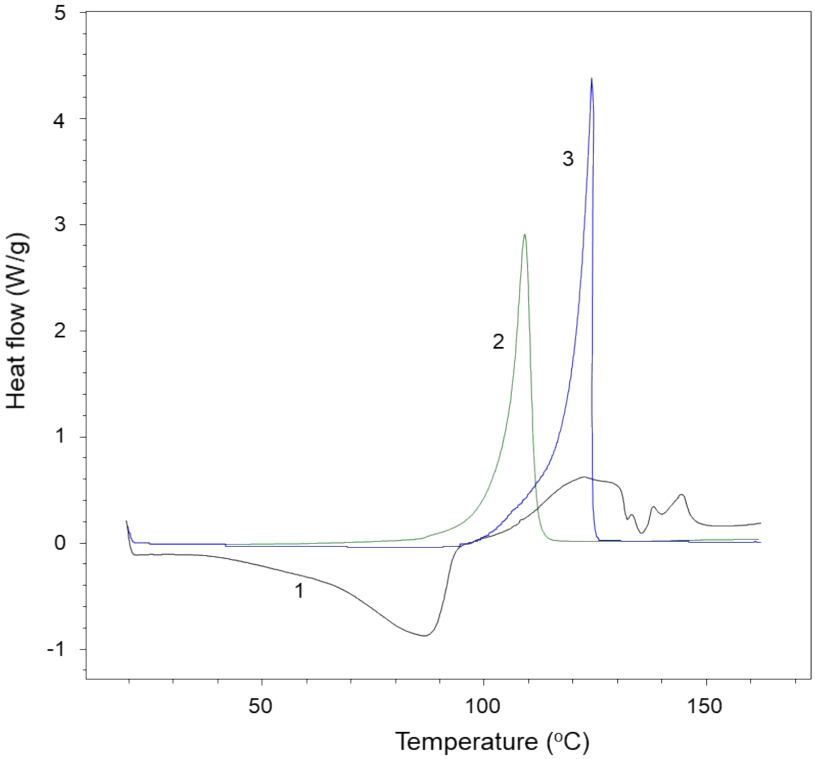

Figure S7. DSC curves of **1**-**3** at 5°C/min heat rate.

The temperature dependent stability of the **1-3** was characterized by differential scanning calorimetry (Figure S3). The melting point of **1** is 88°C. The broad exothermic peak starting at 104 and peaking at 122°C for **1**, corresponds to decomposition of HPCA. The sharp exothermic peak starting at 88 and 90°C and peaking at 109 and 128°C for **2** and **3** respectively correspond to decomposition of corresponding peroxides with release of oxygen and, probably, oxidation reactions of organic fragments.

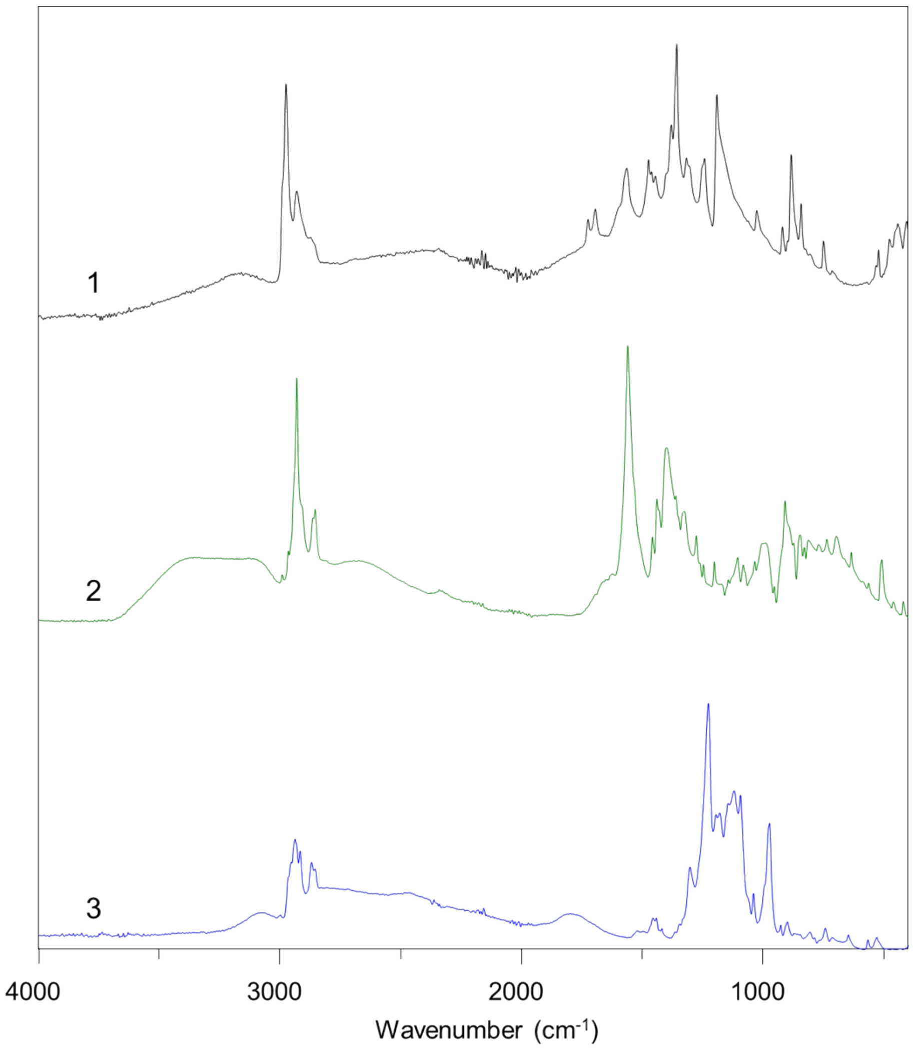

Figure S8. FTIR spectra of **1-3**.

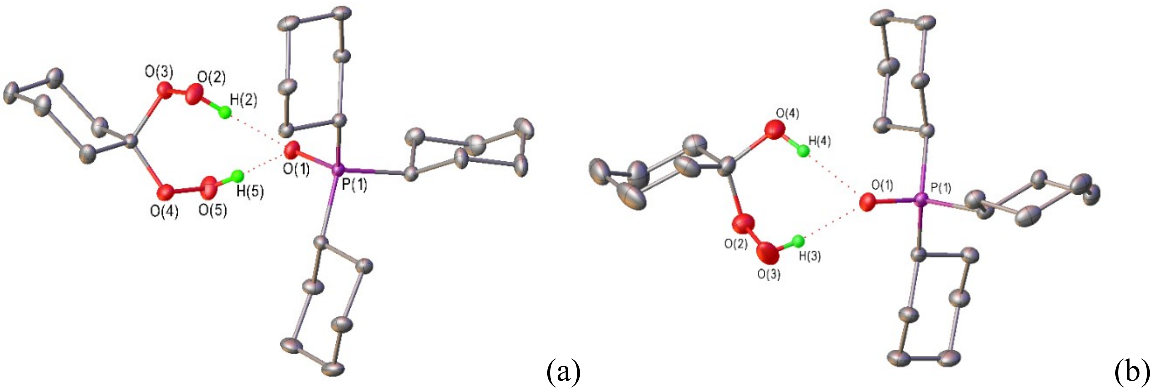

(a) (b)

Figure S9. Asymmetric unit of **4**, REDTAY (a) and **5**, XILRUI (b). H atoms of cyclohexyl substituents are omitted for clarity. Displacement ellipsoids are drawn at the 50% probability level. H-bonds are shown as dashed lines.

References

1 A. O. Terent’ev, M. M. Platonov, Y. N. Ogibin and G. I. Nikishin, *Synth. Commun.*, 2007, **37**, 1281.

2 G. M. Sheldrick, *SADABS ver. -2016/2 - Bruker AXS area Detect. scaling Absorpt. Correct. Progr.*, 2016, Bruker AXS, Karlsruhe, Germany.

3 G. M. Sheldrick, *Acta Crystallogr., Sect. C: Struct. Chem.*, 2015, **71**, 3.

4 R. Dovesi, A. Erba, R. Orlando, C. M. Zicovich-Wilson, B. Civalleri, L. Maschio, M. Rérat, S. Casassa, J. Baima, S. Salustro and B. Kirtman, *WIREs Comput. Mol. Sci.*, 2018, **8**, e1360.

5 J. Laun and T. Bredow, *J. Comput. Chem.*, 2021, **42**, 1064.

6 S. A. Katsyuba, M. V. Vener, E. E. Zvereva, Z. Fei, R. Scopelliti, J. G. Brandenburg, S. Siankevich and P. J. Dyson, *J. Phys. Chem. Lett.*, 2015, **6**, 4431.

7 A. O. Surov, A. N. Manin, A. P. Voronin, A. V. Churakov, G. L. Perlovich and M. V. Vener, *Cryst. Growth Des.*, 2017, **17**, 1425.

8 M. V. Vener, A. V. Churakov, A. P. Voronin, O. D. Parashchuk, S. V. Artobolevskii, O. A. Alatortsev, D. E. Makhrov, A. G. Medvedev and A. Filarowski, *Molecules*, 2022, **27**, 717.

9 Á. M. Montaña, A. Corominas, J. F. Chesa, F. García and M. Font-Bardia, *Eur. J. Org. Chem.*, 2016, **2016**, 4674.

10 H. Osseili, K. N. Truong, T. P. Spaniol, D. Mukherjee, U. Englert and J. Okuda, *Chem. - Eur. J.*, 2017, **23**, 17213.

11 J. L. Flippen-Anderson, *Acta Crystallogr., Sect. C: Struct. Chem.*, 1987, **43**, 2228.

12 S. H. Ahn, N. Bhuvanesh and J. Blümel, *Chem. - Eur. J.*, 2017, **23**, 16998.

13 R. W. Jiang, Y. Wang, H. Gao, D. M. Zhang and W. C. Ye, *J. Mol. Struct.*, 2009, **920**, 383.

14 S. H. Ahn, D. Lindhardt, N. Bhuvanesh and J. Blümel, *ACS Sustainable Chem. Eng.*, 2018, **6**, 6829.

15 Y. Mori and K. Maeda, *Bull. Chem. Soc. Jpn.*, 1994, **67**, 1204.

16 W. Argyrakis, C. Köppl, H. J. Werner, W. Frey, A. Baro and S. Laschat, *J. Phys. Org. Chem.*, 2011, **24**, 682.

17 W. V. Kandur, K. J. Richert, C. J. Rieder, A. M. Thomas, C. Hu, J. W. Ziller and K. A. Woerpel, *Org. Lett.*, 2014, **16**, 2650.

18 X. T. Wang, W. B. Han, H. J. Chen, Q. Zha and Y. Wu, *J. Org. Chem.*, 2020, **85**, 10007.

19 A. V. Churakov, L. G. Kuz’mina, P. V. Prikhodchenko and J. A. K. Howard, *Acta Crystallogr., Sect. E: Struct. Rep. Online*, 2006, **62**, o2265 (6).

20 C. Chen, H. Zhu, X. N. Li, J. Yang, J. Wang, G. Li, Y. Li, Q. Tong, G. Yao, Z. Luo, Y. Xue and Y. Zhang, *Org. Lett.*, 2015, **17**, 644.

21 V. Smyrniotopoulos, A. Quesada, C. Vagias, D. Moreau, C. Roussakis and V. Roussis, *Tetrahedron*, 2008, **64**, 5184.

22 H. M. Li, X. J. Chen, D. Luo, M. Fan, Z. J. Zhang, L. Y. Peng, X. De Wu, R. T. Li, X. Ji and Q. S. Zhao, *Chem. Biodiversity*, 2017, **14**, e1700452.

23 N. D. H. Gamage, B. Stiasny, J. Stierstorfer, P. D. Martin, T. M. Klapötke and C. H. Winter, *Chem. Commun.*, 2015, **51**, 13298.

24 F. F. Arp, R. Ashirov, N. Bhuvanesh and J. Blümel, *Dalton Trans.*, 2021, **50**, 15296.

25 D. C. Haagenson, G. R. Lief, L. Stahl and R. J. Staples, *J. Organomet. Chem.*, 2008, **693**, 2748.

26 Y. Zhang, S. Tong and M. X. Wang, *Angew. Chem., Int. Ed. Engl.*, 2020, **59**, 18151.

27 H.-D. Becker and V. Langer, *Z. Kristallogr. - Cryst. Mater.*, 1993, **206**, 121.

28 B. C. Yan, W. G. Wang, D. B. Hu, X. Sun, L. M. Kong, X. N. Li, X. Du, S. H. Luo, Y. Liu, Y. Li, H. D. Sun and J. X. Pu, *Org. Lett.*, 2016, **18**, 1108.

29 A. V. Yatsenko, V. A. Tafeenko, K. A. Paseshnichenko, T. V. Stalnaya and S. L. Solodar, *Z. Kristallogr. - Cryst. Mater.*, 1998, **213**, 466.

30 B. D. Neisen, N. L. Gagnon, D. Dhar, A. D. Spaeth and W. B. Tolman, *J. Am. Chem. Soc.*, 2017, **139**, 10220.

31 F. F. Arp, S. H. Ahn, N. Bhuvanesh and J. Blümel, *New J. Chem.*, 2019, **43**, 17174.

32 I. A. Guzei and K. C. Miles, *Acta Crystallogr., Sect. C: Struct. Chem.*, 2016, **72**, 179.

33 R.Cherney, M.Eastgate, S.Prasad, Zili Xiao and Michael Yang, *U.S.Patents*, 2008.

34 A. G. Tskhovrebov, E. Solari, R. Scopelliti and K. Severin, *Organometallics*, 2014, **33**, 2405.

35 S. H. Ahn, K. J. Cluff, N. Bhuvanesh and J. Blümel, *Angew. Chem., Int. Ed. Engl.*, 2015, **54**, 13341.

36 S. Parsons, F. Mackay and P. Sadler, *CSD Commun., 2015*, DOI: 10.5517/cc1jfb4f.

37 J. A. Rudd, C. E. Housecroft, E. C. Constable and J. A. Zampese, *CSD Commun.*, 2018, DOI: 10.5517/ccdc.csd.cc207d9z.

38 F. F. Arp, N. Bhuvanesh and J. Blümel, *Inorg. Chem.*, 2020, **59**, 13719.

39 C. Pettinari, F. Marchetti, A. Cingolani, A. Drozdov and S. Troyanov, *Chem. Commun.*, 2000, 1901.

40 W. Uhl, M. R. Halvagar and M. Claesener, *Chem. - Eur. J.*, 2009, **15**, 11298.